https://doi.org/10.1007/s11467-022-1175-0

RESEARCH ARTICLE

Ferroelectricity in hBN intercalated double-layer graphene

Yibo Wang[1,*,†], Siqi Jiang[1,*], Jingkuan Xiao[1], Xiaofan Cai[1], Di Zhang[1], Ping Wang[1], Guodong Ma[1], Yaqing Han[1], Jiabei Huang[1], Kenji Watanabe[2], Takashi Taniguchi[2], Yanfeng Guo[4], Lei Wang[1,3], Alexander S. Mayorov[1,‡], Geliang Yu[1,3,§]

[1] *National Laboratory of Solid State Microstructures and School of Physics, Nanjing University, Nanjing 210093, China*
[2] *National Institute for Materials Science, 1-1 Namiki, Tsukuba 305-0044, Japan*
[3] *Collaborative Innovation Centre of Advanced Microsctructures, Nanjing University, Nanjing 210093, China*
[4] *School of Physical Science and Technology, Shanghai Tech University, Shanghai 201210, China*
Corresponding authors. E-mail: †yibowang@nju.edu.cn, ‡mayorov@nju.edu.cn, §yugeliang@nju.edu.cn
**These authors contributed equally to this work.*
Received January 11, 2022; accepted March 11, 2022

Supporting Information

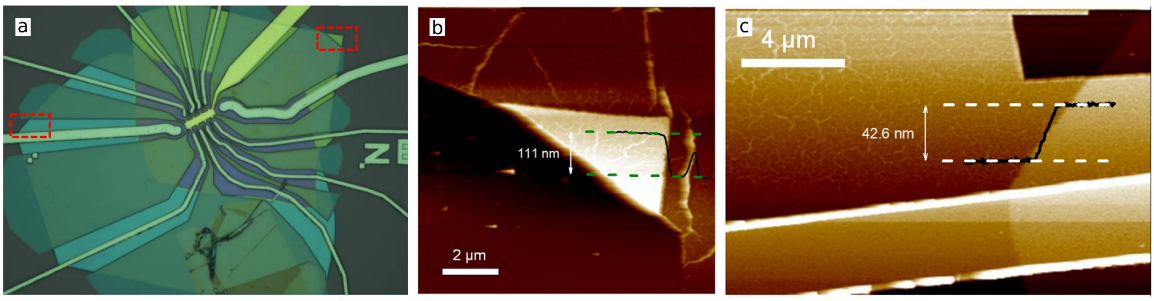

Figure 1. Sample characterisation by AFM a. optical image of the device. The red areas demonstrate the regions for AFM scans. b. Height profile for bottom hBN. c. height profile for the top hBN.

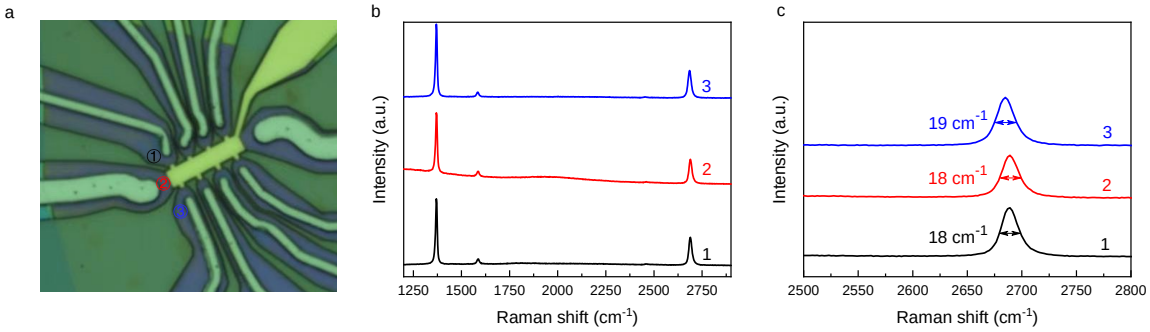

Figure 2. Sample characterisation by Raman spectroscopy a. Optical image of the device with laser spots positions. b. Raman spectra for the selected positions. c. The 2D peak FWHM for different spots.

1 Atomic force microscopy

AFM measurements are performed with a Bruker Dimension Fastscan system at tapping mode. Scan area of bottom/top BN are shown in the right/left red dotted boxes in Fig. 1a. A line cut taken across the bottom/top BN shows a step height of 111 nm and 42.6nm respectively.

2 Raman spectroscopy

Room temperature Raman scattering is performed using a WITec/alpha 300R confocal microscope with 532-nm laser under ambient conditions. The laser power was kept below 1 mW to avoid damage or heating. The G and 2D peaks in the Raman spectra are fitted Lorentzians. Typical Raman spectra of different positions of the heterostructure are plotted in Fig.2b. It is not possible to distinguish the thickness of middle layer BN because its intensity is 50 times smaller than for bulk BN under the same measurement condition[1]. Only monolayer graphene is detected featured by sharp 2D peaks and I(2D)/I(G) ranging from 4.8 to 5.9[2]. Misalignment between graphene and h-BN lattices could be detected by the Raman spectrum using broadening of 2D peak. Nevertheless, the obtained results are in agreement with large angle rotation[3].

3 Geometrical gate capacitance

The relative dielectric constant of hBN, ε_{BN}, is about 5. Therefore, the total capacitance of the bottom gate and graphene can be calculated from series capacitances of two dielectric layers using the following expression

$$C_b = \frac{\varepsilon_{BN}\varepsilon_{SiO_2}\varepsilon_0 S}{\varepsilon_{SiO_2} d_b + \varepsilon_{BN} d_{SiO_2}}, \tag{1}$$

where $\varepsilon_0 = 8.854 \times 10^{-12}$ F/m is the vacuum permittivity (), ε_{SiO_2} is dielectric constant of SiO_2 (3.9), d_{SiO_2} and d_b are thicknesses of SiO_2 and bottom BN respectively. The thickness of bottom BN is determined by AFM. It is equal to 111 nm. S is the area of the device. The relation between the concentration and the gate voltage can be calculated by

$$n = \frac{C_b V_{bg}}{eS} = \frac{\varepsilon_{BN}\varepsilon_{SiO_2}\varepsilon_0}{\varepsilon_{SiO_2} d_b + \varepsilon_{BN} d_{SiO_2}} \frac{V_{bg}}{e}, \tag{2}$$

where e is the elementary charge. The coefficient of proportionality between n and the V_{bn} is equal to 5.58×10^{14} $\mathrm{m^{-2}V^{-1}}$.

For the top gate the lever arm is equal to 6.5×10^{15} $\mathrm{m^{-2}V^{-1}}$.

4 Mean free path

The mean free path can be found from

$$l = \frac{\hbar}{e}\sqrt{\pi n}\mu, \tag{3}$$

where μ is the mobility, which is equal in both layers and independent on concentration. In the case of approximately equal separation of the charge carriers in both graphene layers one can expect mean free path in a single layer of $l_g = l/\sqrt{2}$. The sample width is equal to 2.7μm, which corresponds to the 60 $\mathrm{m^2V^{-1}s^{-1}}$ at $n_{tot} = 3 \times 10^{15}\mathrm{m^{-2}}$, 42 $\mathrm{m^2V^{-1}s^{-1}}$ at $n_{tot} = 6 \times 10^{15}\mathrm{m^{-2}}$, and 35 $\mathrm{m^2V^{-1}s^{-1}}$ at $n_{tot} = 9 \times 10^{15}\mathrm{m^{-2}}$. The estimated values are larger than the observed low-temperature mobilities by 30%.

5 Temperature dependence of the resistivity

Here we present the temperature dependence of the resistivity for for the forward (Fig.3a) and backward sweeps (3b) of V_{bg} at $V_{tg} = 0$V. The temperature changes from 2K to 325K. The resistivity does not change sometimes gradually but demonstrates jumps in the position of the charge neutrality point (CNP). Nevertheless the difference between the positions of the CNPs for the backward and forward sweeps is reducing with increasing temperature and does not disappear up to the highest available temperature for our cryostat (325K).

6 Top gate sweeps

To show robustness of the hysteresis at low temperature we used top gate sweeps at fixed back gate voltages. The resulting maps are shown in Fig.4.

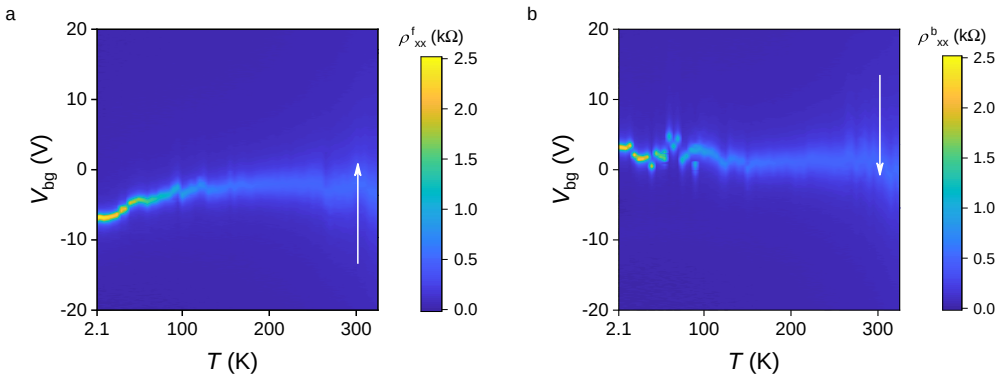

Figure 3. Temperature dependence of the resistivity a. Forward sweep. b. backward sweep.

7 Paraelectric phase

The sample shows a paraelectric behaviour after thermal cycling. The temperature was raised above room temperature, and then the sample was cool down to the base temperature (2.1K). The ferroelectric effect disappeared, as shown in Fig.5. The forward and backward sweeps for the resistivity maps do not show hysteretical behaviour.

8 Two types of carries

Generally, two graphene layers have different concentrations of the charge carries independently of the gate voltage appplied. The conductivity tensor in Drude model will be a combination of two parallel channels and can be described by 2D antisymmetric tensor:

$$\sigma_{ij} = \begin{bmatrix} \sigma_{xx} & \sigma_{xy} \\ -\sigma_{xy} & \sigma_{xx} \end{bmatrix}, \tag{4}$$

where

$$\sigma_{xx} = \frac{e_t n_t \mu_t}{1+\mu_t^2 B^2} + \frac{e_b n_b \mu_b}{1+\mu_b^2 B^2}, \tag{5}$$

$$\sigma_{xy} = \frac{e_t n_t \mu_t^2 B}{1+\mu_t^2 B^2} + \frac{e_b n_b \mu_b^2 B}{1+\mu_b^2 B^2}. \tag{6}$$

Here, indexes t and b correspond to the top and bottom layers, respectively. The particle charge, concentration, mobility are determined by e, n, μ respectively with the layer index. In our experiment we are dealing with resistivity so inversion of the conductivity tensor gives the following expression

$$\rho_{ij} = \begin{bmatrix} \rho_{xx} & \rho_{xy} \\ -\rho_{xy} & \rho_{xx} \end{bmatrix} = \sigma_{ij}^{-1} = \frac{1}{\sigma_{xx}^2+\sigma_{xy}^2} \begin{bmatrix} \sigma_{xx} & -\sigma_{xy} \\ \sigma_{xy} & \sigma_{xx} \end{bmatrix}, \tag{7}$$

where the independent elements of the resistivity matrix are given by

$$\rho_{xx} = \frac{\sigma_t + \sigma_b + (\sigma_t \mu_d^2 + \sigma_b \mu_t^2) B^2}{(\sigma_t+\sigma_b)^2 + (\sigma_t^2 \mu_b^2 + \sigma_b^2 \mu_t^2) B^2}, \tag{8}$$

$$\rho_{xy} = -\frac{(\sigma_t \mu_t + \sigma_b \mu_b) B + (\sigma_t \mu_b + \sigma_b \mu_t) \mu_t \mu_d B^3}{(\sigma_t+\sigma_b)^2 + (\sigma_t^2 \mu_b^2 + \sigma_b^2 \mu_t^2) B^2}, \tag{9}$$

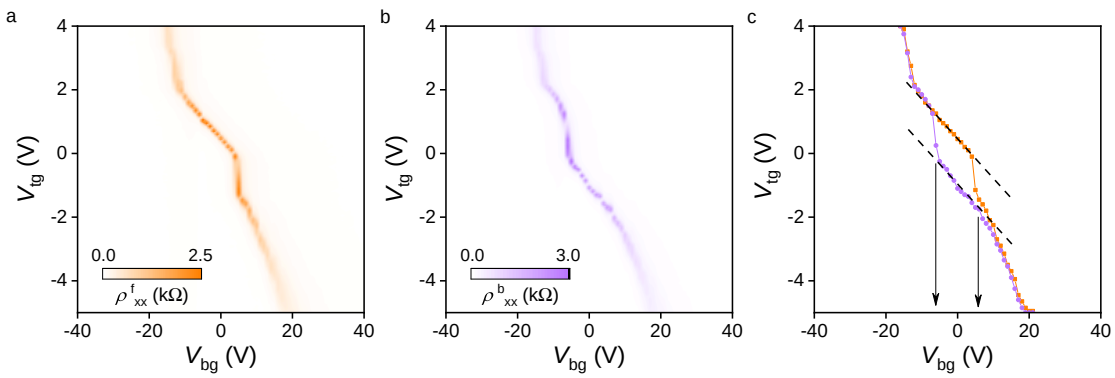

Figure 4. Ferroelectric hysteresis at 2.1K. (**a**-**b**) The sample's resistivity as a function of the top gate and bottom gate voltages for the forward (**a**) and backward (**b**) top gate voltage sweeps at fixed V_{bg}. **c**. The maximum of the resistivity for the forward (black squares) and backward (red circles) as a function of the top gate and back gate voltages. The dashed line is the best fit for the forward and backward sweeps' resistivity maxima in the linear ferroelectric regime.

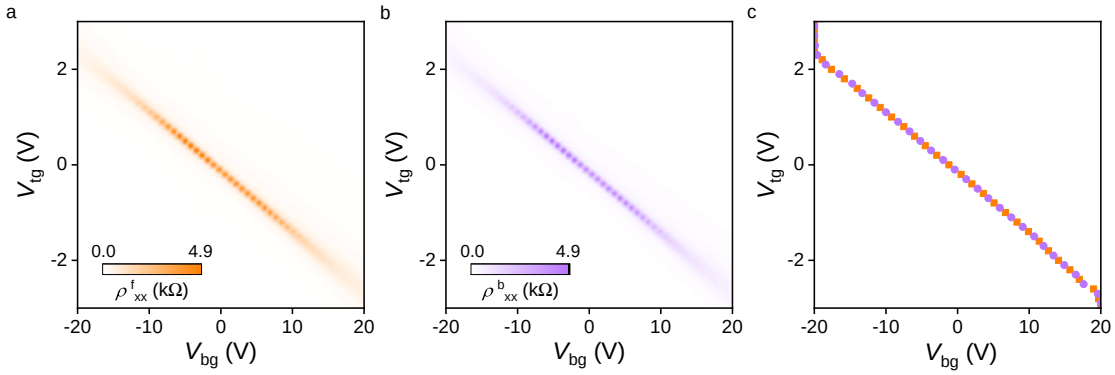

Figure 5. Paraelectric phase at 2.1K. (**a**-**b**) The sample's resistivity as a function of the top gate and bottom gate voltages for the forward (**a**) and backward (**b**) top gate voltage sweeps at fixed V_{bg}. **c**. The maximum of the resistivity for the forward (black squares) and backward (red circles) as a function of the top gate and back gate voltages.

where we introduced the following notation for the conductivities of the top and bottom layers at zero magnetic field $\sigma_t = e_t n_t \mu_t$ and $\sigma_b = e_b n_b \mu_b$, respectively. In the case of different charge carriers the charge will change the sign and the mobility will charge the sign accordingly.

In the case of identical mobility for both layers (and the same charge) the conductivity tensor is the same as it would be for one layer.

9 Another ferroelectric state

The sample was warmed up after the normal state was restored. Then after two weeks, stored at room temperature, the sample was cool down again. The new ferroelectric state was revealed in a new set of measurements is shown in (Fig.6). The new ferroelectric state is observed at low temperatures. The sample's resistance demonstrates hysteresis as a function of back gate and top gate. The hysteresis demonstrates temperature dependence, and its area decreases with increasing temperature, as shown in Fig.6a,b. The effect disappears above 150 K (Fig.6c) and converts to a paraelectric phase. To confirm the memory effect, the resistance as a function of top gate voltage is measured at 2.1K. The sweep of top gate voltage was made to demonstrate high- and low-resistance states in Fig.6d.

There is no convincing theory behind the observation of different ferroelectric and paraelectric phases in our sample, so we could only speculate on the qualitative origin of these phases. A thin BN layer placed on graphene can slide[4,5] to form a superlattice with different alignment regions between C-atoms in both graphene layers and B and N atoms. Mechanical stress-induced, in this case, should be in favour of the formation of slight periodic variations of strain. This additional energy has to affect the total free energy of the structure and cause slight variations on the B and N atoms displacement in the z-direction. This should cause different ferroelectric phases that characterise different displacement field distributions. Of course, there should be many different realisations of such scenarios; however, we cannot discriminate them from the data presented here.

References

1. Gorbachev, R. V. *et al.* Hunting for monolayer boron nitride: Optical and raman signatures. *Small* **7**, 465–468, DOI: https://doi.org/10.1002/smll.201001628 (2011).

2. Ferrari, A. C. *et al.* Raman spectrum of graphene and graphene layers. *Phys. Rev. Lett.* **97**, 187401, DOI: https://link.aps.org/doi/10.1103/PhysRevLett.97.187401 (2006).

3. Eckmann, A. *et al.* Raman fingerprint of aligned graphene/h-bn superlattices. *Nano Lett.* **13**, 5242–5246, DOI: https://doi.org/10.1021/nl402679b (2013).

4. Woods, C. R. *et al.* Charge-polarized interfacial superlattices in marginally twisted hexagonal boron nitride. *Nat. Commun.* **12**, 347, DOI: https://doi.org/10.1038/s41467-020-20667-2 (2021).

5. Stern, M. V. *et al.* Interfacial ferroelectricity by van der waals sliding. *Science* **372**, 1462–1466, DOI: https://doi.org/10.1126/science.abe8177 (2021).

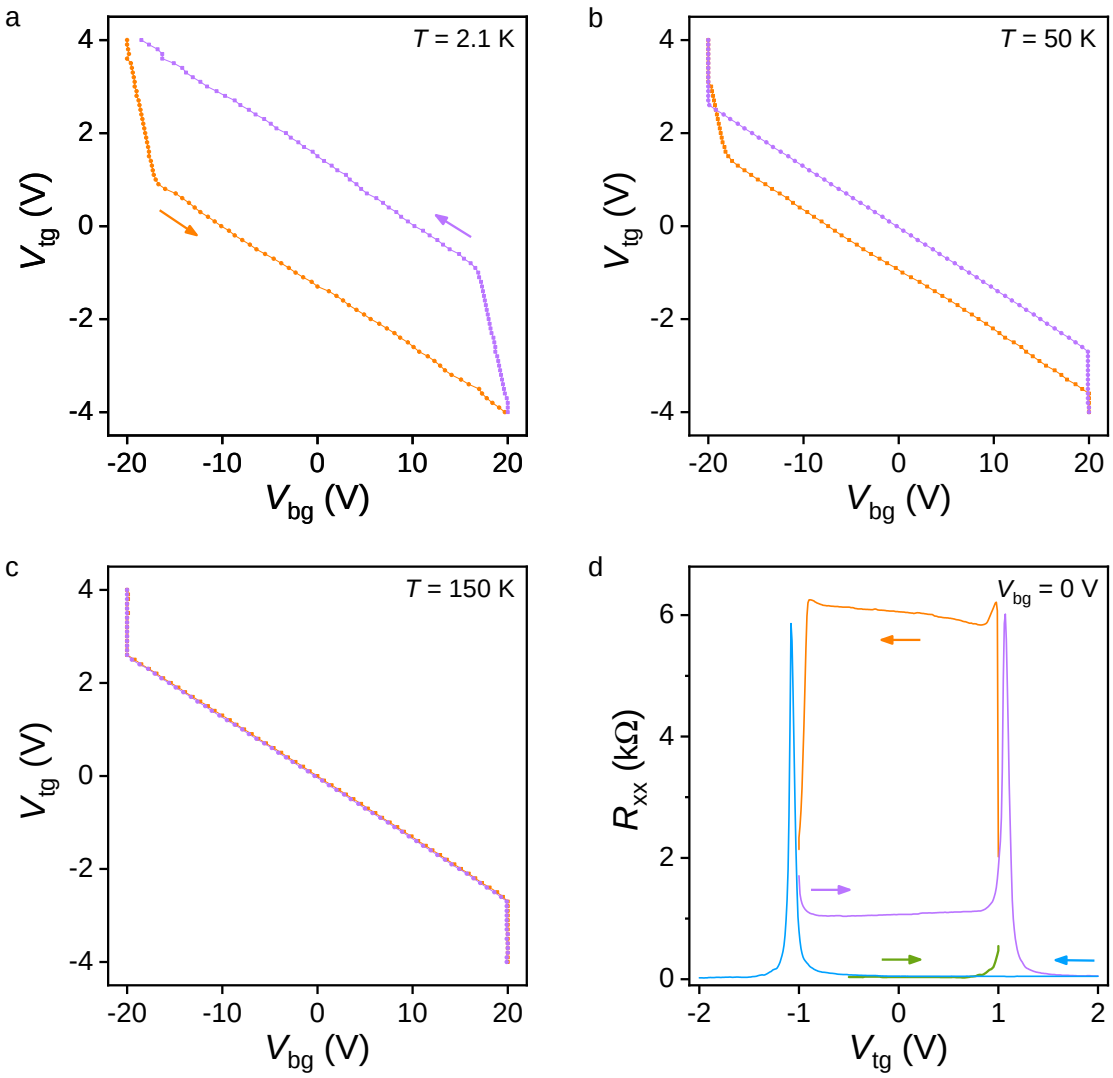

Figure 6. Second ferroelectric state (**a**-**b**) The resistivity maximum for forward (**a**) and backward (**b**) back gate voltage sweeps at the fixed top gate for 2.1 K and 50 K respectfully. Orange and purple squares indicate forward and backward sweeps, respectively. **c**. Maximum resistance as a function of top and back gate voltages for the forward and backward sweeps at T=150K. **d**. Resistance as a function of top gate voltage is shown by the following sequence green - orange - purple - blue.